# HYSTERESIS MODELING WITH PRANDTL-ISHLINSKII OPERATORS FOR LINEARIZATION OF A (BA/SR)$TIO_3$ BASED ACTUATOR

Andreea Ioana UDREA[1], Alexandru COSTINOAIA[2], Ciprian LUPU[3], Dumitru POPESCU[4]

*Lucrarea prezintă un studiu experimental având ca element principal comportamentul histeretic al unui element de execuţie ce utilizează materialul (Ba,Sr)$TiO_3$. Scopul studiului este modelarea neliniarităţii introduse de elementul de execuţie într-un sistem de pozitionare. Metodele Prandtl – Ishlinskii clasică şi modificată sunt folosite pentru a permite controlul sistemului de poziţionare pe baza unui compensator care conţine modelul invers al elementului. Comportamentul histeretic a fost modelat pentru domeniul de functionare normal si extins. Pentru ambele cazuri au fost obtinute modele bune şi compensatorul bazat pe modelul invers a dus la o bună liniarizare a efectului neliniar introdus de elementul de acţionare.*

*The paper presents an experimental study on (Ba,Sr)$TiO_3$ based actuators hysteretic comportment. The purpose of the study is to model the nonlinearity introduced by the actuator in a positioning system. The classic and modified Prandtl – Ishlinskii technique is used such that the numerical control of the positioning system could also be achieved, by using the inverse model of the actuator. The hysteretic comportment of the actuator was modeled for the normal and extended functioning domain. In both cases the models are accurate and the inverted model based compensators provide good linearization of the effect introduced by the actuator.*

**Keywords:** hysteretic nonlinearity model, numerical compensator

## 1. Introduction

Although sustained efforts to eliminate or at least reduce the effects of hysteresis phenomena onto controlled systems were made during the last decades, the traditional control approaches seem insufficient. In the present, the attention to

[1] Assistant, Faculty of Automatic Control and Computers, University POLITEHNICA of Bucharest, Romania
[2] Eng., Faculty of Automatic Control and Computers, University POLITEHNICA of Bucharest, Romania
[3] Reader, Faculty of Automatic Control and Computers, University POLITEHNICA of Bucharest, Romania
[4] Prof., Faculty of Automatic Control and Computers, University POLITEHNICA of Bucharest, Romania, e-mail: andreea, calex, cip, dpopescu@indinf.pub.

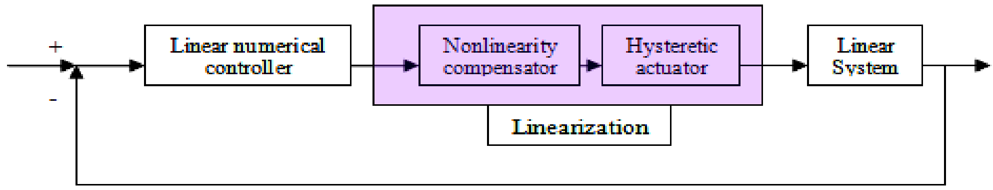


Fig. 1. Positioning control with hysteresis linearization by means of inverse model compensator

the subject increased due to the large number of applications that confront with this aspect.

One of the problems concerning hysteresis is that there are a lot of ways of modeling it, but the approach is purely phenomenological and the models are difficult to work with from real-time control applications point of view.

Lately, there appeared a series of models like the Prandtl – Ishlinskii [1], [2] model that are very appealing for numerical control. They have a series of limitations concerning the compensator design due to non inversability of the model for control under different conditions (small intervals between thresholds, not positive defined slope of the hysteretic curve, singularity for negative or zero weights), but, in spite of these, they are viable solutions for most of the applications confronting with this type of nonlinearity.We want to determine the applicability of this solution to eliminate the hysteretic effect introduced by a Ba/$SrTiO_3$ based actuator in a positioning system.

Ba/$SrTiO_3$ is a piezoceramic material with hysteretic proprieties largely investigated in the last 10 year. It is used for: oxygen sensors, actuators, magnetic memories, capacitors in microwave applications, etc.

The hysteretic effect of the material is modeled. The nonlinearity is reduced in a simple feed forward structure using the inversed model compensator positioned before de actuator (linearization block in figure 1). The linear part of the system can be classically controlled like in figure 1. where the controller can be of various types: PID, RST, etc.

The small error resulting from the linearization can be viewed as a perturbation for the control system and must be taken into consideration when designing an enough robust controller.

## 2. Hysteretic Nonlinearities. Modeling and control using PI operators

The Prandtl-Islinskii model for the hysteretic characteristic consists in a weighted superposition of backlash operators (hysterons). Each operator is described by a weight and a magnitude: $w_i$ and $r_i$ – figure 2. a):

The discretization of the relations proposed by Kuhnen [3], [4] are presented next. The backlash operator is defined by the recurrent relation:

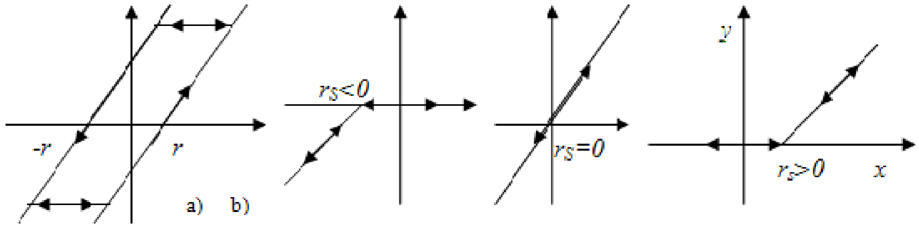


Fig. 2. a) Backlash operator; b) one side dead zone operators

$$y(k\cdot T_s) = H_{rH}[x(k\cdot T_s), z_0] = \max\{x(k\cdot T_s) - r_H, \min\left(x(k\cdot T_s) + r_H, y\left((k-1)T_s\right)\right\} \quad (1)$$

The hysteresis model fig. 2.a) can be written as:

$$H[x(kT_s)] = \sum_{i=0}^{n} w_i H_{ri}[x(kT_s), z_{0i}] \quad (2)$$

where:

- $k = 0.. N$, $t_0 = 0$ and $t_E = kT_s$; $T_s$ - sampling period and $N+1$ sampled $x$-$y$ data are used;
- $n$ - is the order of the model;
- weights vector - $w^T = (w_0, w_1, \ldots, w_n)$;
- magnitudes vector - $r^T = (r_0, r_1, \ldots, r_n)$ with $0 = r_0 < r_1 < \ldots < r_n < \infty$;
- initial states vector - $z_0{}^T = (z_{00}, z_{01}, \ldots, z_{0n})$;
- backlash operator vector - $H_{r_H}^T[x, z_0](t) = (H_{r_{H0}}^T[x, z_{00}](t), \ldots, H_{r_{Hn}}^T[x, z_{0n}](t))$.

For the numerical implementation of the algorithm, the following steps must be done:

1. Select the magnitudes for the backlash operators, usually equal; and, for simplicity, the initial conditions 0:

$$r_i = \frac{i}{n+1} \max_k\{|x(k\,T_s)|\,;\quad z_{0i} = 0. \quad (3)$$

2. Determine the weights by minimizing (4). A quadratic minimization criterion is used. There is one solution, assuring the invariability of the model.

$$\min_w\{w^t\Omega^t\Omega w\},\quad \Omega = \begin{bmatrix} H_{r_0}[x(0), z_{00}] & \cdots & H_{r_n}[x(0), z_{0n}] \\ H_{r_0}[x(T_s), z_{00}] & \cdots & H_{r_n}[x(T_s), z_{0n}] \\ \vdots & \ddots & \vdots \\ H_{r_0}[x(k\,T_s), z_{00}] & \cdots & H_{r_n}[x(k\,T_s), z_{0n}] \end{bmatrix}_{n+1} \quad (4)$$

under the restriction:

$$U \cdot w - u \geq 0 \qquad U = \begin{bmatrix} 1 & 0 & . & 0 & 0 \\ 1 & 1 & . & 0 & 0 \\ . & . & . & . & . \\ . & . & . & 1 & 0 \\ 1 & 1 & . & 1 & 1 \end{bmatrix}_{n+1} \qquad u = \begin{bmatrix} \varepsilon \\ \varepsilon \\ . \\ . \\ \varepsilon \end{bmatrix}_{n+1}$$

Once the vectors $w$, $r$, $z_o$ are known, the hysteretic model $H$ of order $n$ is given by relation (2).

3. For the inverted model, first, $w'$ is obtained from the formulas:

$$w'_0 = \frac{1}{w_0}, \quad w'_i = -\frac{w'_i}{(w_0 + \sum_{l=1}^{i} w_l)(w_0 + \sum_{l=1}^{i-1} w_l)} \tag{5}$$

In order to determine $z'$ the next relation is used: $z'_{0t} = \sum_{l=0}^{i} w_l z_{oi} + \sum_{l=0}^{i} w_l z_{ol}$

For $r'$ the following transformation is made: $r'_i = \sum_{l=0}^{i} w_l (r_i - r_l)$.

The inverted model, $H^{-1}$ - that gives the compensator is:

$$H^{-1}[y(kT_s)] = \sum_{i=0}^{n} w'_i H_{r'_i}[y(kT_S), z'_{oi}] \tag{6}$$

The steps leading to an efficient numerical model and compensator of a hysteretic nonlinearity, easy to implement for real-time applications was presented. This is called the Prandtl-Ishlinskii model and is recommended for hysteretic curves with symmetry - due to the superposition of backlash operators (symmetric). For more complex hysteretic nonlinearities (asymmetric curves), the modified Prandtl-Ishlinskii model is better suited. This model overcomes the restrictions by using one-side dead zone operators, figure 2. b), characterized by the threshold $r_S$ and with the capability of catching the asymmetric features of the loops:

$$S[x, r_S] = \begin{cases} \max\{x - r_S, 0\}, & r_S > 0 \\ x, & r_S = 0 \\ \min\{x - r_S, 0\}, & r_S < 0 \end{cases} \tag{7}$$

These new operators are superposed on the backlash operators and the discrete model is obtained [5] :

$$\Gamma[x(kT_s)] = \sum_{i=-m}^{m} w_{Sj}^T S_{r_{Sj}} [\sum_{i=0}^{n} w_{Hi}^T H_{r_{Hi}} [x(kT_s), z_{H0i}]] \quad (8)$$

where:

- in the brackets - $H_{rHi}$ stands for a the corresponding backlash operator value at the specified moment;
- $n$ – the number of backlash operators; $2m+1$ - the number of dead zone operators; $n+2m+1$ – the order of the model;
- $w_H$ / $w_S$ weights vector (dimension n/2m+1) for backlash/dead zone operators;
- $r_H$ / $r_S$ magnitudes vector(dimension n/2m+1) for backlash/dead zone operators.

The implementation of the numerical algorithm, in this case, must follow the next steps:

1. Initialization of the magnitudes; like in the previous algorithm, equal values and initial conditions equal to 0, were consider :

$$r_{H_i} = \frac{i}{n+1} \max_k\{|x(k\,T_s)|\} \quad \text{and} \quad z_{0i} = 0 \quad (9)$$

For the dead zone magnitudes, the algorithm starts with choosing the inverted values this way: for $j$ equaling $0;$ between $1$ and $m$, respectively between $-m$ and $-1$, the relations are:

$$r'_{S0} = 0\,;\quad r'_{Si} = \frac{(j-\frac{1}{2})}{m} \max_k[y(k\,T_s)]\,;\quad r'_{Si} = \frac{(j+\frac{1}{2})}{m} \min_k[y(k\,T_s)] \quad (10)$$

2 . The solution for the following problem under restrictions must be solved to determine $w = \begin{bmatrix} w_H \\ , \\ w_S \end{bmatrix}$. The optimization problem is over determined with one degree of freedom, because both operators - in the positions with magnitudes 0, $H_{r_H}|_{r_H=0}$ and $S_{r'_S}|_{r'_S=0}$, are equal to the identity operator $I$. The equality in (11) anoles this supplementary degree and assures the unicity of the solution for the quadratic minimization problem.

$$\min_w\{w^t \Omega^t \Omega w\}\,,\ \begin{bmatrix} U_H & 0 \\ 0 & U_S \end{bmatrix} \cdot \begin{bmatrix} w_H \\ w_S \end{bmatrix} - \begin{bmatrix} u_H \\ u_S \end{bmatrix} \leq 0 \ \text{and} \ \left( [\|x\|_\infty \cdot I - r_H)^T \quad 0^T] \cdot \begin{bmatrix} w_H \\ w'_S \end{bmatrix} \right) - \|x\|_\infty = 0 \quad (11)$$

where:

$$w_H = \begin{bmatrix} w_{h0} \\ w_{h1} \\ .. \\ w_{hn} \end{bmatrix} \quad w'_S = \begin{bmatrix} w'_{s(-m)} \\ .. \\ w'_{s0} \\ .. \\ w'_{sm} \end{bmatrix} \quad U_S = \begin{bmatrix} -1 & .. & -1 & -1 & 0 & .. & 0 \\ .. & .. & .. & -1 & .. & .. & .. \\ 0 & .. & -1 & -1 & 0 & .. & 0 \\ 0 & .. & 0 & -1 & 0 & .. & 0 \\ 0 & .. & 0 & -1 & -1 & .. & 0 \\ .. & .. & .. & -1 & .. & .. & .. \\ 0 & .. & 0 & -1 & -1 & .. & -1 \end{bmatrix}_{(2\cdot m+1)}$$

$$u_H = \begin{bmatrix} -\varepsilon \\ 0 \\ .. \\ 0 \end{bmatrix}_{n+1} \quad u_S = \begin{bmatrix} -\varepsilon \\ -\varepsilon \\ .. \\ -\varepsilon \end{bmatrix}_{2m+1} \quad U_H = -I_{n+1} \quad I = \begin{bmatrix} 1 \\ 1 \\ .. \\ 1 \end{bmatrix}_{n+1}$$

The acquired *x*-*y* data are used to form the following matrix *HH* and *SS*:

$$HH = \begin{bmatrix} H_{r_{Ho}}[x(0), z_{00}] \ldots H_{r_{Hn}}[x(0), z_{0n}] \\ H_{r_{Ho}}[x(T_s), z_{00}] \ldots H_{r_{Hn}}[x(0), z_{0n}] \\ \vdots \quad \ddots \quad \vdots \\ H_{r_{Ho}}[x(kT_s), z_{00}] \ldots H_{r_{Hn}}[x(kT_s), z_{0n}] \end{bmatrix}_{(k+1)x(n+1)}$$

$$SS = \begin{bmatrix} -S'_{r_{s(-m)}}[y(0)] & \ldots -S'_{r_{s0}}[y(0)] & \ldots -S'_{r_{sm}}[y(0)] \\ -S'_{r_{s(-m)}}[y(T_s)] & \ldots -S'_{r_{s0}}[y(T_s)] & \ldots -S'_{r_{sm}}[y(T_s)] \\ \vdots \quad \ddots & \vdots \quad \ddots & \vdots \\ -S'_{r_{s(-m)}}[y(kT_s)] & \ldots -S'_{r_{s0}}[y(kT_s)] & \ldots -S'_{r_{sm}}[y(kT_s)] \end{bmatrix}_{(k+1)x(2m+1)}$$

$$\Omega = [HH \ \ SS]_{(k+1)x(n+1+2n+1)}$$

3. The values of $w_S$ and $r_S$ vectors for the positive indexes $i = 1..m$:

$$r'_{Si} = \sum_{j=0}^{i} w_{Sj}(r_{Si} - r_{Sj})$$

$$w'_{S0} = \frac{1}{w_{S0}} \ ; \ w'_{Si} = -\frac{w_{Si}}{\left(w_{S0} + \sum_{j=1}^{i} w_{Sj}\right)\left(w_{S0} + \sum_{j=1}^{i-1} w_{Sj}\right)}$$

leading to:

$$r_{S0} = 0 \ ; \ r_{Si} = \frac{r'_{si} + \sum_{j=1}^{i-1} w_{sj} \cdot r_{sj}}{\sum_{j=1}^{i-1} w_{sj}} \qquad (12)$$

$$w_{S0} = \frac{1}{w'_{S0}} \; ; \; w_{Si} = -\frac{w'_{Si}(w_{S0} + \sum_{j=1}^{i-1} w_{Sj})^2}{1 + w'_{Si}(w_{S0} + \sum_{j=1}^{i-1} w_{Sj})}$$

For the negative indexes $i = -m..-1$:

$$r'_{Si} = \sum_{j=i}^{-1} w_{Sj}(r_{Si} - r_{Sj})$$

$$w'_{S0} = \frac{1}{w_{S0}} \; ; \; w'_{Si} = -\frac{w_{Si}}{(w_{S0} + \sum_{j=i}^{-1} w_{Sj})\,(w_{S0} + \sum_{j=i+1}^{-1} w_{Sj})}$$

and it results:

$$r_{S0} = 0 \; ; \; r_{si} = \frac{r'_{si} + \sum_{j=i+1}^{-1} w_{sj} \cdot r_{sj}}{\sum_{j=i+1}^{-1} w_{sj}}$$

$$w_{S0} = \frac{1}{w'_{S0}} \; ; \; w_{Si} = -\frac{w'_{Si}(w_{S0} + \sum_{j=i+1}^{-1} w_{Sj})^2}{1 + w'_{Si}(w_{S0} + \sum_{j=i+1}^{-1} w_{Sj})} \quad (13)$$

Using the above results, the hysteresis mathematical model - $\Gamma$ - can be written as relation (8).

4. For the inverted model - $\Gamma^{-1}$ - :

$$\Gamma^{-1}[y(kT_s)] = \sum_{i=0}^{n} w'^{T}_{Hi} H_{r'_{Hi}} [\sum_{j=-m}^{m} w'^{T}_{Sj} S_{r_{Sj}} [y(kT_s), z'_{H0i}]] \quad (14)$$

with $k= 0..N$ and $r'_H$, $w'_H$ and $z'_{H0}$ to be determined from:

$$r'_{Hi} = \sum_{j=0}^{i} w_{Hj}(r_{Hi} - r_{Hj}) \; cu \; i = 0 \ldots n$$

$$w'_{H0} = \frac{1}{w_{H0}} \; ; \; w'_{Hi} = \frac{1}{(w_{H0} + = \sum_{j=0}^{i} w_{Hj}) \cdot (w_{H0} + = \sum_{j=0}^{i-1} w_{Hj})}$$

$$z'_{H0i} = \sum_{j=0}^{i} w_{Hj} \cdot z_{H0i} + \sum_{j=i+1}^{n} w_{Hj} \cdot z_{H0j} \quad (15)$$

The mathematical methods for determining the model and the inverted model based compensator using the direct and modified Prandtl-Ishlinskii operators, previously presented, were developed in Matlab 2008.

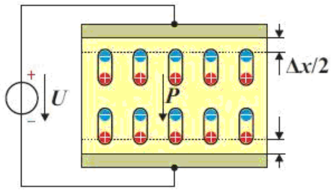

Fig. 3. Inverse piezoelectric effect

The data are loaded from the acquisition files; the classic and modified PI – model and the inverse model routines for both cases can be selected; a series of test routines containing different generated signals to be tracked are used to calculate the algorithms performances in terms of quadratic tracking error.

The number of data is relevant in terms of model exactitude. The larger the data set (smaller sampling period for acquisition) the better the model.

It must be observed that the model order is also important, usually there is a lower and upper limit for which the model is acceptable, by depassing a certain order does not lead to better performances, while the operations per sampling period increase.

The routines were developed to be used for any kind of hysteretic data and produce the model and numerical compensator for both symmetric and asymmetric curves, graphically display the interest measures and test the compensator for different input signals. In the next chapter, a case study on a $(Ba,Sr)TiO_3$ based actuator is performed.

## 3. Case study - $(Ba,Sr)TiO_3$ based actuators

### 3.1. Data aquisition

The used data were obtained by applying an electric field on the piezoceramic de titanat de 0.6 bariu/ 0.4 strontiu ( $Ba/SrTiO_3$ ) probe and measuring the polarization. The polarization is directly proportional with the displacement (order of micrometers) so, in the absence of an accurate displacement measuring device, the measured polarization value will be considered: $P=e/\Delta x$, where $P$ is the polarization; $e$ is the piezoelectric coefficient of the material and $\Delta x$ is the displacement.

The hysteretic comportment of the actuator was measured for input tensions that lead to a symmetric hysteretic characteristic - where the errors introduced by the nonlinearity are small figure 4. c) and, also, for input values that lead to an asymmetric hysteretic curve (figure 4.f) ) and implicitly to larger errors.

In the second case – figure 4 d) ,e) ,f) - the problem of extending the functioning domain for the material is considered. Increasing the polarization leads to larger displacements. An asymmetric characteristic is obtained due to the integral orientation of the ferroelectric domains after the direction of the applied electrical field.

In figure 4 the profound nonlinear characteristic of the actuator under a triangular command signal can be observed. The differences between the two cases (normal/extended functioning domain) are given by the (a)symmetry when considering the first bisector.

The data were acquired after the period when the loading curve was traversed. The sampling period was of 30 ms and 400 *x*-*y* pairs of data were stored for each measurement.

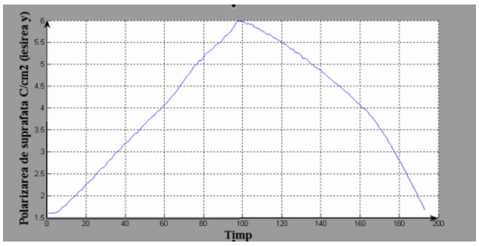


a) generator command (time[s] vs. surface polarization[C/cm$^2$])

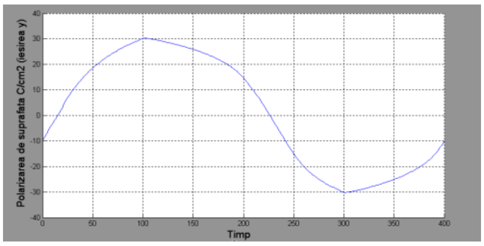


d) generator command (time[s] vs. surface polarization[C/cm$^2$])

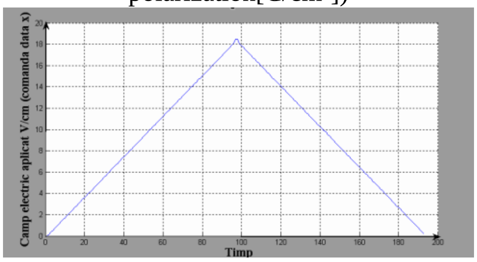


b) probe output (time[s] vs. applied electrical field[V/cm])

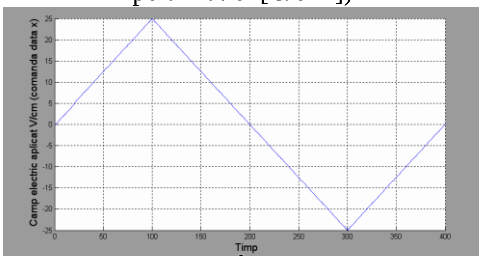


e) probe output (time[s] vs. applied electrical field[V/cm])

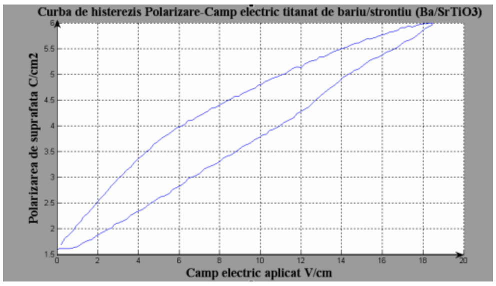


c)hysteretic characteristic - for the minor / narrow ferroelectric loop (surface polarization[C/cm$^2$] vs. applied electrical field[V/cm])

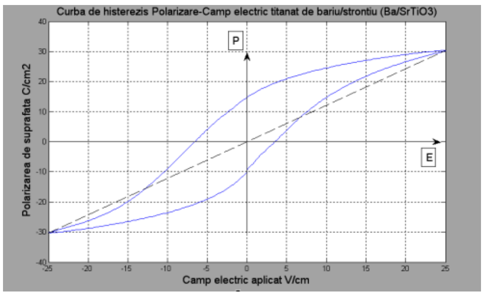


f) hysteretic characteristic – for the major ferroelectric loop (surface polarization[C/cm$^2$] vs. applied electrical field[V/cm])

Fig. 4. a), b), c) - normal functioning domain; d), e), f) - extended functioning domain

### 3.2 Symmetric hysteretic curve modeled with PI backlash operator superposition

Considering the first case, where the hysteretic curve is symmetric due to the application of a positive electric field such that the reorientation of all the ferroelectric domains is not complete (unsaturated) - the curve evolution was presented in fig. 3.

For this model, due to the symmetry, the superposition of backlash operators alone had been used. The models order is 16 (although good results were obtained starting with order 8) and 400 data were used to determine it.

In fig. 5.a), the measured curve is plotted in red and the obtained model in blue. It can be observed that a good approximation has been achieved; the differences are greater in the upper region where the curve is not perfectly symmetric relatively to the first bisector. In fig. 5.b) the model and the inverted model (giving the compensator) that is used to eliminate the nonlinearity are presented. The performances of the compensator were tested by tracking the reference curve (red) that consists in two sinusoidal signals with different amplitudes and frequencies. The output of the system is plotted in blue in fig. 4.c).

A quadratic error of 1.13%. has been obtained. The numerical effort per step is less then 10ms.

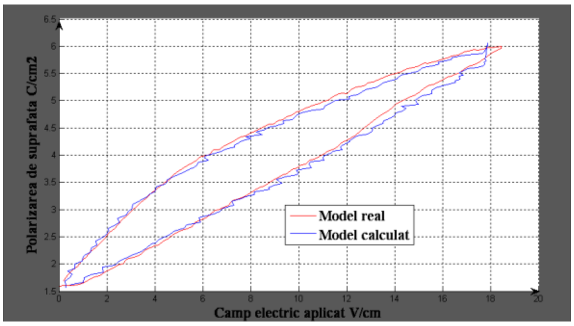


Fig. 5.a Real characteristic(red) vs Model(blue) (surface polarization[C/cm$^2$] vs. applied electrical field[V/cm])

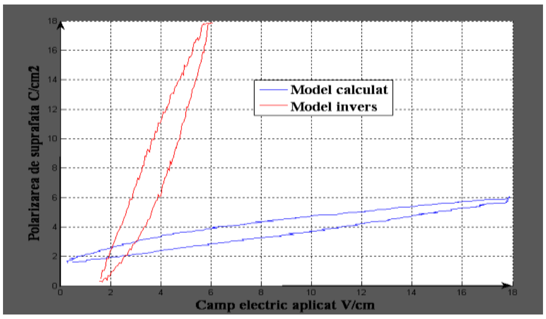


Fig. 5.b Model(blue) inverted model(red) (surface polarization[C/cm$^2$] vs. applied electrical field[V/cm])

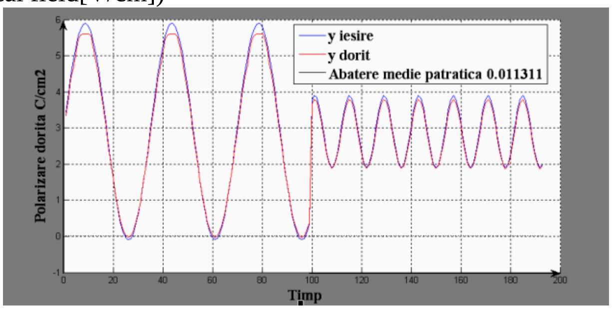


Fig. 5.c Probe signal for tracking(red) vs. (blue) Compensated actuator output (polarization[C/cm$^2$] vs. time[s])

### 3.2 **Symmetric hysteretic curve modeled with PI backlash operator superposition and saturation operators.**

This part of the paper refers to the hysteretic comportment of the material when extending the functioning domain. Higher values of the polarization and implicitly higher displacement are obtained. In figure 4. f), it can be observed that the nonlinearity is more pronounced and asymmetric relatively to the first bisector.

First, the model was created by using only backlash operators. In a second phase, the model is created using both backlash and dead zone operators. The two models and the obtained compensators performances will be compared.

For the first model, 16 backlash operators were used. In figure 7. a) the difference between the model and the measured data is significant. The asymmetry can not be captured by the symmetric backlash operators.

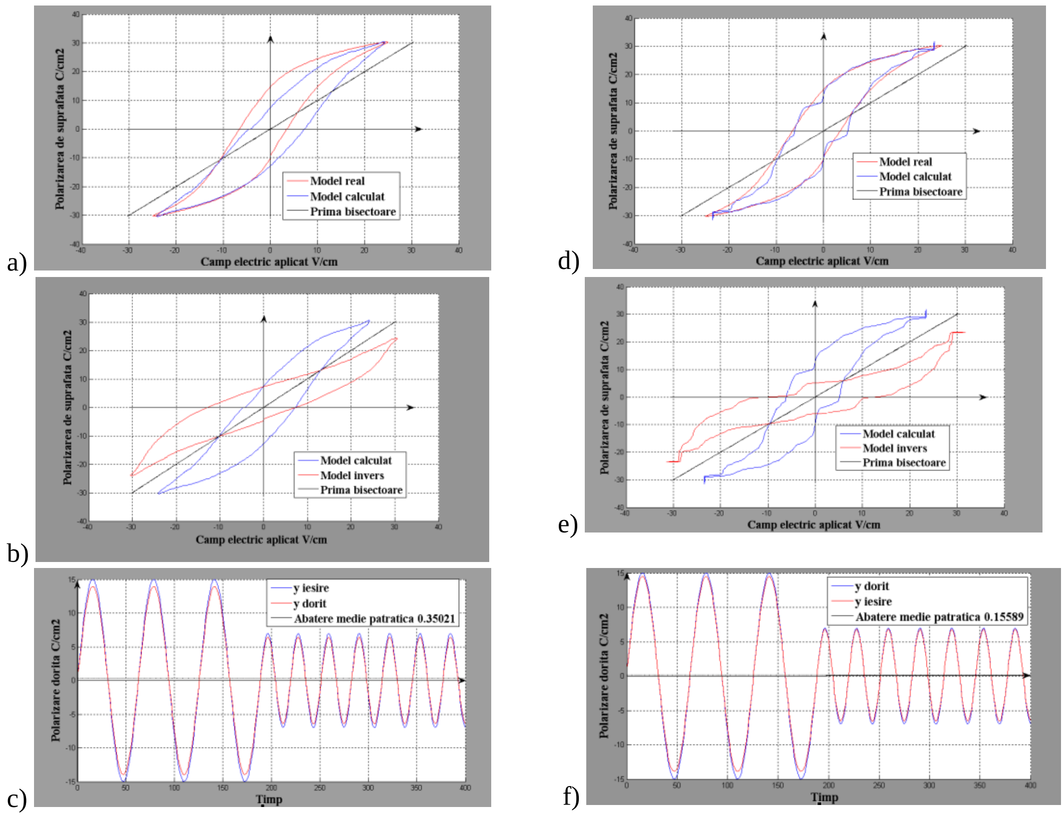


Fig. 7. Asymmetric characteristic – backlash operators only: a) Real characteristic(red) vs. Model(blue) b) Model(blue) inverted model(red) c) Probe signal for tracking(red) vs. (blue) Compensated actuator output; Asymmetric characteristic – backlash and dead zone operators: d) Real characteristic vs. Model e) Model inverted model f) Probe signal for tracking vs. Compensated actuator output.

Increasing the order of the model does not improve the results. The compensator designed based on this model reduce the tracking error – figure 6 c), but the error is larger than 3.5%

For the second model, 15 backlash operators and 10 dead zone operators has been used – the complexity of the model was almost doubled. The modeling results improved – the asymmetry was captured by the asymmetric dead zone operators. Increasing their number leads to improved results, but increases the amount of operations that must be done on each sampling period, this way decreasing the numeric robustness of the compensator. The trajectory was better pursuit. The tracking error was reduced to 1.5%.

## 4. Conclusions

This paper proposes an algorithm for modeling the hysteretic comportment of a $Ba/SrTiO_3$ based piezoelectric actuator (normal and extended functioning domain) and eliminates the nonlinearity introduced by it in a positioning system. The model and inverted model used for the compensator is determined off-line using Prandtl-Ishlinskii methods. Once calculated, the inverted model in the compensator needs a small number of operations – function of the models' order - to calculate the value that leads to the linearization of the actuator dynamics. Once integrated in a real time control application, the tracking error was diminished from more than 20% to under 2% in both cases. By further increasing the orders of the model, the error couldn't be diminished and the number of operations on a sampling period would be increased without any reason.

**Acknowledgement**

This work was partially supported by CNCSIS - IDEI Program of Romanian Research, Development and Integration National Plan II, Grant no. 1044/2007.

## B I B L I O G R A P H Y

[1] *Q. Wang, C. Su,* Robust adaptive control of a class of nonlinear systems including actuator hysteresis with Prandtl–Ishlinskii presentations, Automatica, vol. 42, 2006, pp 859 – 867
[2] *Y.W. Park, Y.T. Seok, H.J. Park, J.Y. Chung*, Hysteresis modeling based on saturation operator without constraints, Journal of Magnetism and Magnetic Materials, 2007, 2647–2649
[3] *P. Krejcí, K. Kuhnen*, Inverse control of systems with hysteresis and creep, IEE Proc.-Control Theory Appl., Vol. 148, **No. 3**, 2001,185-192.
[4] *K. Kuhnen, H. Janocha,* Inverse feedforward controller for complex hysteretic nonlinearities in smart-material systems, Proc. of the 20th IASTED-Conf. on Modeling, Identification and Control, Insbruck, 2001, 375-380
[5] *J. Shen, W. Jywea, H. Chiang, Y. Shub*, Precision tracking control of a piezoelectric-actuated system, Science Direct, Precision Engineering 32, 2008, 71–78.